

Fracturing and deformation in the Chicxulub crater – Complex trace analysis of instantaneous seismic attributes

Eduardo Salguero-Hernández¹, Jaime Urrutia-Fucugauchi^{1,*}, and Luis Ramírez-Cruz²

¹ Proyecto Universitario de Perforaciones en Océanos y Continentes, Instituto de Geofísica, Universidad Nacional Autónoma de México, Delegación Coyoacán, 04510 México D.F., Mexico.
Present address: Instituto Mexicano del Petróleo, Avenida de los Cien Metros, México D.F., Mexico.

² Instituto Mexicano del Petróleo, Avenida de los Cien Metros, México D.F., México.

* juf@geofisica.unam.mx

ABSTRACT

Large complex impact craters form by collapse from initial excavation stage of a deep narrow bowl-shaped transient cavity. Fracturing and shattering of solids with finite tensile shear limits occur related to shock-induced damage of target material, with fracturing and fragmentation occurring during transient cavity crater collapse processes. Geophysical studies of subsurface crater structure may assist in studying shock-induced effects of deformation and fracturing of target rocks. Here we present initial results of a study of subsurface fracturing/deformation in the Chicxulub crater from seismic reflection data. The analysis is based on the instantaneous seismic attributes envelope amplitude, instantaneous frequency and Q factor, at selected sectors of the crater by looking at petrophysical properties and seismic attenuation. Shock effects with shattering and fracturing of Mesozoic target rocks show a trend to decrease away from the rim zone. Cretaceous carbonates show less attenuation inside the crater than in exterior sectors. The relative attenuation quality factor Q is lower in sections outside the crater rim as compared with higher Q values inside the rim, and particularly at depth within the Cretaceous sequence. Carbonates in the western sector are characterized by slightly larger attenuation than in the eastern sector, suggesting radial asymmetries in fracturing/deformation within Chicxulub.

Key words: cratering, geophysical modeling, instantaneous seismic attributes, Chicxulub crater, Mexico.

RESUMEN

Los cráteres de impacto complejos se forman por colapso a partir de la etapa inicial de excavación de una cavidad transitoria más profunda y en forma de cuenca. El fracturamiento de las rocas de la zona de impacto está asociado a los efectos inducidos por el choque, con fracturamiento y deformación vinculados al colapso de la cavidad transitoria. Estudios geofísicos de la estructura profunda del cráter permiten investigar los efectos inducidos por el choque en las rocas de la zona de impacto. En este trabajo presentamos los resultados iniciales del estudio de la deformación y fracturamiento en el cráter de Chicxulub utilizando datos marinos de sismología de reflexión. Los análisis están basados en la determinación de los atributos sísmicos instantáneos de envolvente de amplitudes, frecuencia instantánea

y factor Q , en sectores seleccionados del cráter, analizando las propiedades petrofísicas y la atenuación sísmica. Los efectos de choque en el fracturamiento y deformación de la secuencia carbonatada mesozoica muestran una tendencia a disminuir fuera de la zona central del anillo. La secuencia de carbonatos del Cretácico muestra menor atenuación dentro del cráter que en las zonas exteriores. El factor de atenuación Q es menor en las secciones fuera del cráter en comparación con los altos valores del factor Q dentro de la estructura y en particular a mayor profundidad en la secuencia cretácica. Los carbonatos en el sector oeste se caracterizan por un factor de atenuación ligeramente mayor que el observado en el sector este, lo que apoya los modelos de asimetría radial de la deformación y el fracturamiento de la estructura.

Palabras clave: modelado geofísico, atributos sísmicos instantáneos, cráter de Chicxulub, México.

INTRODUCTION

In the past years, understanding of the characteristics, genesis and evolution of planetary surfaces has increased, partly associated with the availability of high resolution multi-spectral data from space probes and Earth-based observational systems and partly from experimental and theoretical developments of processes acting on the surfaces of planets, satellites, asteroids and comets. One of the major processes in the formation and shaping of planetary surfaces in the solid bodies (inner solar system planets, satellites and asteroids) is impact cratering resulting from cometary and meteorite collisions in a wide range of spatial and temporal scales. Observations on the surfaces of the Moon, Mars, Mercury and other bodies have long documented the occurrence of craters with sizes spanning several orders of magnitude and distinct size-related morphologies from the small simple bowl-shaped basins to large complex central-peak, peak-ring and multi-ring structures (e.g., Melosh, 1989; Urrutia-Fucugauchi and Perez-Cruz, 2009). Analyses of the morphology and inferences from experimental and simulation studies have been used to investigate the mechanisms and factors involved in cratering and to develop models for crater formation. Recently, use of increased computer power and more sophisticated computer codes such as the hydrocode have permitted to test some of these models and to evaluate the role of poorly understood variables in solid fragmentation, cracking and tensile stress regimes (e.g., Melosh *et al.*, 1992; Ahrens and Rubin, 1993; Collins *et al.*, 2008). However, simulations with three-dimensional geometries and realistic impact dynamic parameters and rheological properties of bolide and target materials still present major challenges. Study of large complex craters present additional problems from difficulties in extrapolation of laboratory scale experiments and nonlinear behavior at the high temperatures and pressures involved in high velocity large impacts.

Field observations and experimental and simulation models have indicated different patterns of deformation and fracturing, ranging from little deformed bowl-shaped simple craters to the radial ring-fracture patterns in complex structures. Schematic models for formation of complex craters with central and peak ring morphologies are illustrated in

Figure 1 (Melosh, 1989). Models show part of the complexity of the processes involved in cratering from the initial contact and excavation stages that produced the transient cavity and fragmentation and ejection of target material from different depths to the modification stage with crustal uplift, crater collapse, ejecta emplacement and structural accommodation and faulting. Surface morphology of central-peak, peak-ring, and multi-ring craters indicates significant fracturing of target with formation of radial ring-fracture patterns. Structural complexities of large craters result from crater collapse, and study of the mechanics of crater collapse has provided inferences on the mechanical and rheological

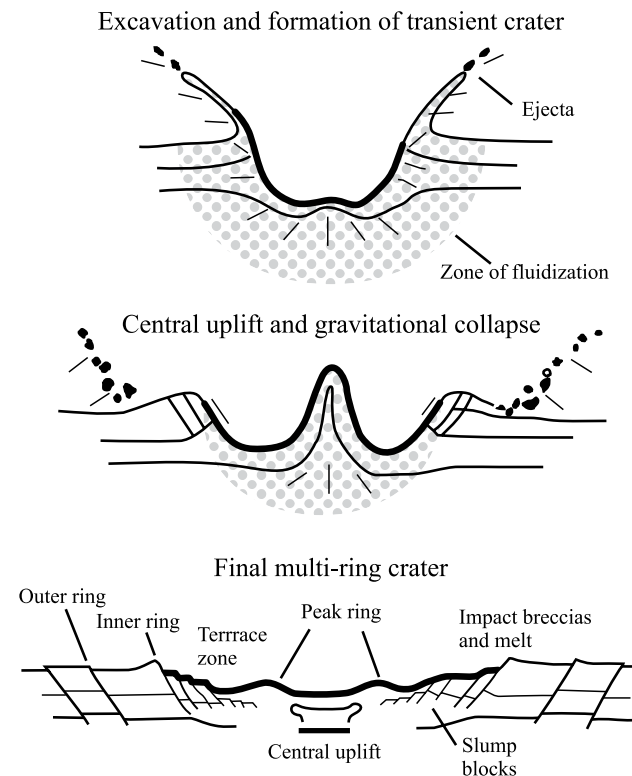


Figure 1. Schematic models for multi-ring crater formation, involving fracturing and deformation of target rock sequence during initial excavation, basement uplift and crater collapse and modification stage. Multi-ring crater morphology involves formation of central uplift, peak ring, terrace zone, slump blocks and inner and outer rings (after Melosh, 1989).

properties of the material and nature of deformation and fracturing (e.g., Melosh and Gaffney, 1983; Melosh and Ivanov, 1999; O'Keefe and Ahrens, 1999).

Crater studies on planetary surfaces from remote observations and space probes are limited to two-dimensional surface observations. Underground studies based on geophysical surveys and drilling are only available for craters on our planet. However, in contrast to the other planetary surfaces, the dynamic environment on Earth with tectonism, volcanism, and weathering has significantly destroyed much of the crater record. There are less than two-hundred impact craters documented on Earth, and from them only three correspond to the large multi-ring structures: Vredefort (South Africa), Sudbury (Canada) and Chicxulub (Mexico) (Grieve and Therriault, 2000; Urrutia-Fucugauchi and Perez-Cruz, 2009). The first two craters were formed in the Precambrian, some 2000 Ma and 1850 Ma ago, and have been significantly affected by tectonic and erosional processes. Chicxulub crater was formed much later at 65 Ma, and the particular stable characteristics of the site where the impact occurred have permitted preservation of much of the crater morphology and impact lithologies. Chicxulub formed on a shallow marine carbonate platform in the southern sector of the Gulf of Mexico and, after impact, carbonate sedimentation covered the structure, and the peninsula has not been affected by tectonic and magmatic activity.

In this paper, we present initial results of a study of subsurface fracturing/deformation associated with the Chicxulub multi-ring crater based on seismic reflection data. Complex trace analysis of seismic attributes has proved a powerful technique in oil exploration, reservoir characteri-

zation and crustal studies. In particular, applications to fractured carbonate sequences permit to investigate attenuation and fracturing. In this study, we use instantaneous seismic attributes to investigate selected crater sectors by looking at the petrophysical properties and seismic attenuation.

CHICXULUB MULTI-RING CRATER

Chicxulub crater is located in the northwestern sector of the Yucatan peninsula, southern Gulf of Mexico, buried under Tertiary carbonate sediments (Figures 2 and 3). The structure was initially documented from the gravity and magnetic anomalies, which showed a roughly circular concentric pattern of gravity anomalies with high amplitude magnetic anomalies in its central zone, suggesting a buried basin under the carbonate sediments. As part of the oil exploration program of the Yucatan peninsula, several exploratory wells were drilled with intermittent core recovery, which documented the stratigraphy and occurrence of igneous-textured rocks within the basin (López-Ramos, 1975). Hildebrand *et al.* (1991) proposed that the structure correspond to an impact crater formed at the Cretaceous/Tertiary (K/T) boundary, which was supported by subsequent studies (e.g., Sharpton *et al.*, 1992; Urrutia-Fucugauchi *et al.*, 1994, 1996; Hildebrand *et al.*, 1998; Rebolledo-Vieyra and Urrutia-Fucugauchi, 2006). Geophysical surveys have been conducted to document the geometry and structure of the crater (e.g., Sharpton *et al.*, 1993; Morgan *et al.*, 1997; Hildebrand *et al.*, 1998; Delgado-Rodríguez *et al.*, 2001; Ortiz-Alemán and Urrutia-Fucugauchi, 2010) and drilling/coring projects (e.g., Urrutia-Fucugauchi *et al.*, 1996,

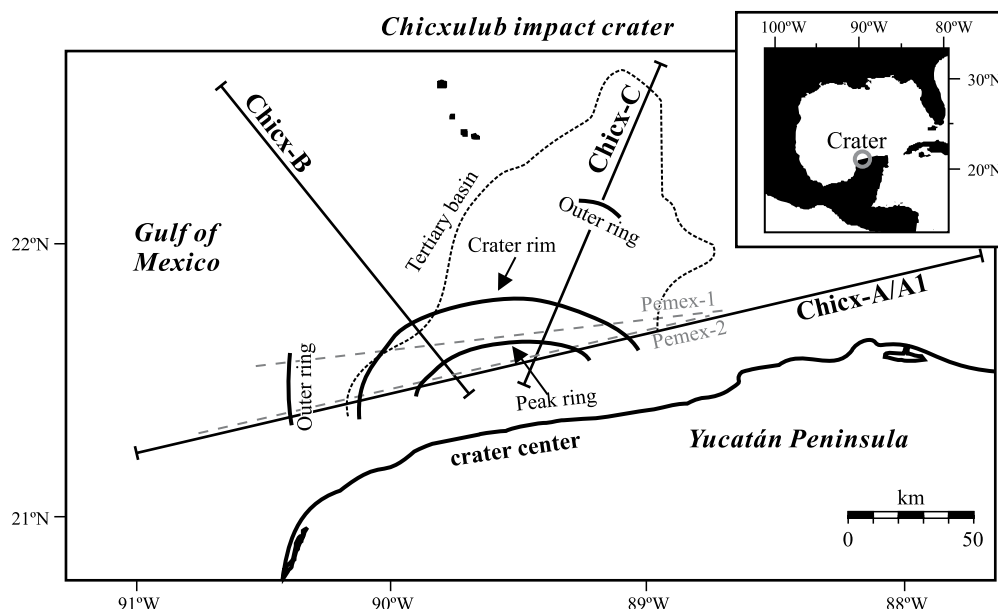


Figure 2. Location of seismic profiles from the Chicxulub Seismic Experiment (taken from Christeson *et al.*, 2001). Profile analyzed is the Chicx-A/A1 crossing the crater structure from the west to east. Sections analyzed are located in the external zone (outward sections) and internal zone (inner sections).

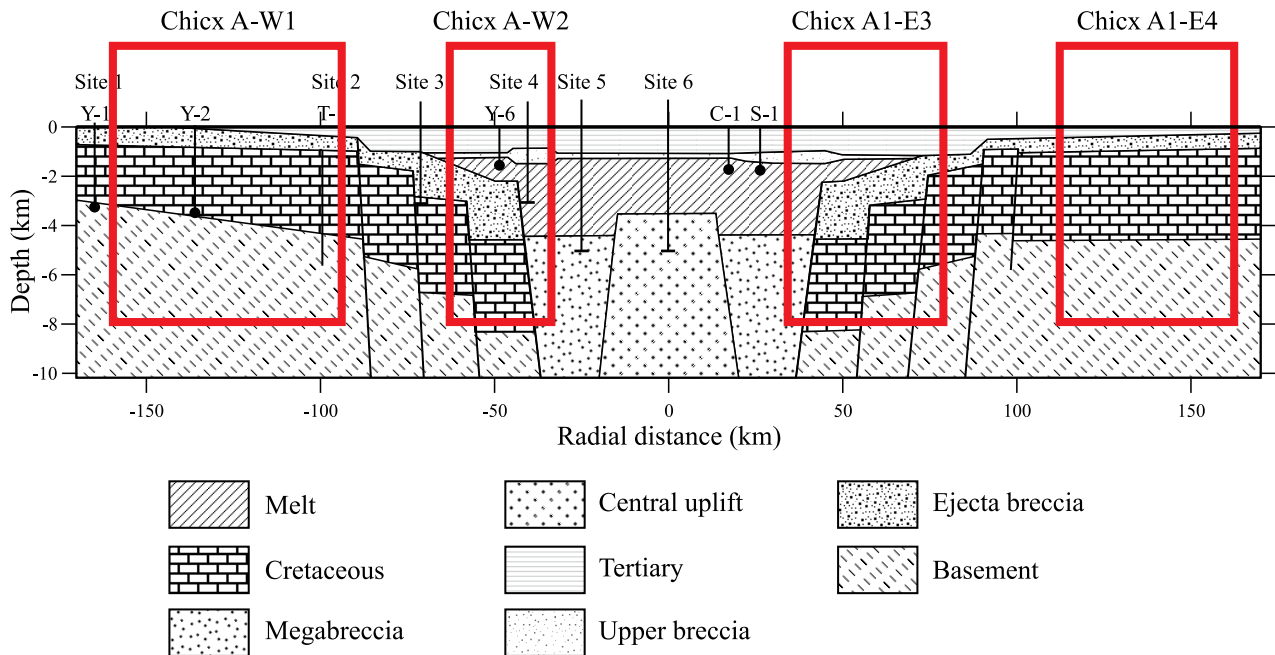


Figure 3. Schematic model of Chicxulub crater, showing major structural units of the Tertiary sequence, central uplift, breccia units, melt sheet, Cretaceous target sequence and basements units. Location of sections analyzed by instantaneous seismic attributes is indicated by the red rectangles, and have been selected for the study of fracturing and attenuation in the target rocks (Cretaceous sequences in the crater model).

2004, 2008; Rebolledo-Vieyra *et al.*, 2000). Potential field anomaly and seismic reflection studies have documented a multi-ring 200 km-diameter structure with a central structural uplift and peak-ring morphology for Chicxulub (*e.g.*, Morgan *et al.*, 1997; Hildebrand *et al.*, 1998; Morgan and Warner, 1999; Christeson *et al.*, 2001).

For this study of deformation and fracturing in the Chicxulub crater, we used seismic reflection data from two long profiles that cross the structure (Figure 4). The profiles Chicx-A and Chicx-A1 are located NW-SE parallel to Yucatan coastline some 20 km offset from its center, which were acquired during the Chicxulub seismic experiment (Morgan *et al.*, 1997). The air gun profiles were acquired at 50m (20s) shot spacing from the GECO SIGMA seismic vessel, which carried a Bolt air gun array with a volume of 150 liters and pressure of 2000 psi. A composite recording streamer with 162 hydrophone groups at 12.5m group spacing and 78 hydrophone groups at 50m spacing. The 36 element air gun array presented a flat response between 8 and 50 Hz. Seismic processing has been presented in previous studies (Morgan *et al.*, 1997; Morgan and Warner, 1999; Christeson *et al.*, 2001; Morgan *et al.*, 2002). Major noise sources were mudroll and peg-leg multiples, coming from waves traveling along the water-sediment interface because of the shallow water depths close to the coast, and strong impedance contrasts within the Cretaceous and also the Tertiary sequences. FK filters applied to shot gathers were used to remove mudroll effects, and two deconvolution processes and inherent velocity filter within stacking were used to reduce the peg-leg multiples. Stacking velocities

come from semblance, mini-stack and trial midpoint gathers that maximized primary reflection coherency. For our initial analysis, we used the processed and filtered stack sections also used for finite-difference time migrations and depth-to-depth conversions supplied by BIRPS and Chicxulub seismic experiment.

The velocity model for profiles Chicx-A and Chicx-A1 constrained by wide-angle data obtained after tomographic inversion is shown in Figure 4. The seismic velocity model documents occurrence of the Tertiary basin characterized by lower velocities of less than 4.5 km/s and the underlying impact units (breccias and melt sheet?) and carbonate Mesozoic section with higher velocities (Christeson *et al.*, 2001).

SEISMIC ATTRIBUTES

From analysis of seismic data and joint interpretations from potential field anomalies, exploratory wells and seismic reflection models (Morgan *et al.*, 1997, 2002; Hildebrand *et al.*, 1998; Christeson *et al.*, 2001; Ortiz-Alemán and Urrutia-Fucugauchi, 2010; Urrutia-Fucugauchi and Pérez-Cruz, 2008), we selected four windows along the profiles for initial study of deformation and fracturing related to shock induced damage in the Mesozoic target sequence, Tertiary sediments and impact lithologies. Major structural features of the crater include the basin depression filled with Tertiary carbonate sediments, the peak ring, the central basement uplift, the terrace zone/slump blocks and

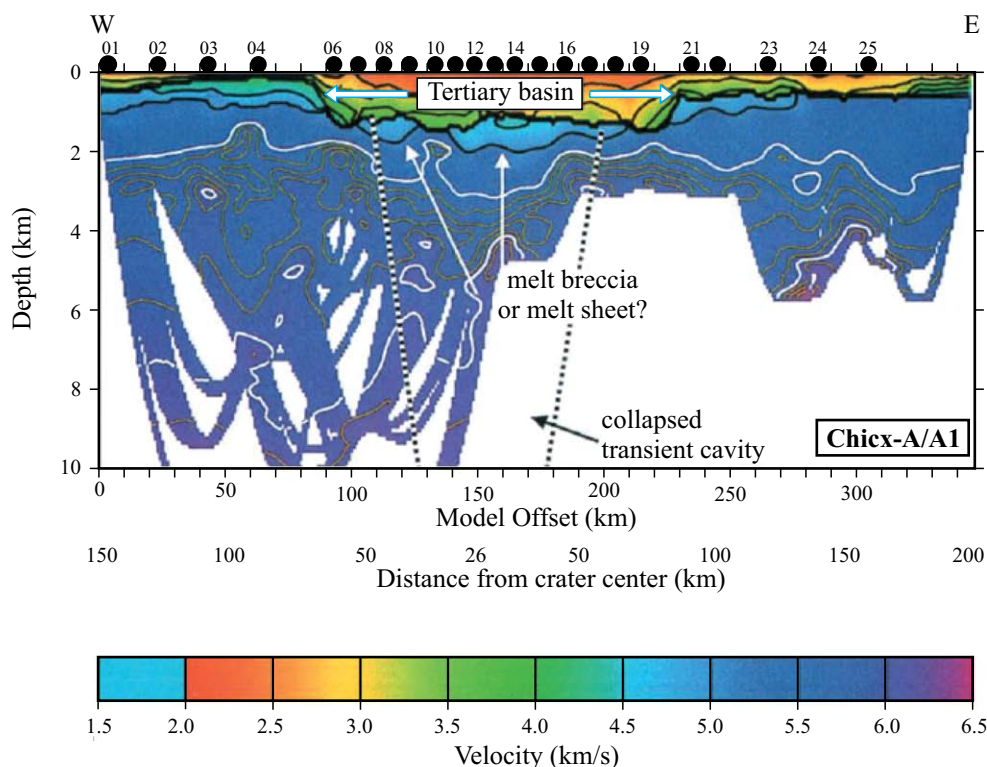


Figure 4. Velocity model for the Chicxulub crater based on the tomographic inversion and ocean bottom seismogram data (adopted from Christeson *et al.*, 2001).

the crater, outer and exterior rings (Figure 3). The peak ring and central deformation zone beneath the Tertiary basin is related to material collapse as modeled by hydrocode simulations (Collins *et al.*, 2008). Major faulting is indicated in the terrace zone, extending from beneath the peak ring to the exterior rim. Inward dipping reflectors corresponding to the crater, outer and exterior rims support fracturing and faulting during cratering.

For the initial analysis, we selected the instantaneous frequency, envelope amplitude and attenuation quality factor Q , which provide a characterization of the petrophysical properties and attenuation characteristics for the sections. Analyses of seismic attributes in oil exploration surveys, reservoir characterization and crustal studies have proved a powerful technique. We have used seismic attributes to study fractured carbonate sequences in northeastern and southern Mexico and tested ways to evaluate attenuation and fracturing in carbonates. The methodology is described by Taner and Sheriff (1977) and Taner *et al.* (1979) (see also Sheriff, 1991; Chopra and Marfurt, 2005). Examples of applications in attenuation analysis is given in Del Valle-García and Ramírez-Cruz (2002) and Ramírez-Cruz *et al.* (2005).

The instantaneous frequency attribute represents the rate of phase change in the seismic wave with time (Taner *et al.*, 1979; Barnes, 1996). Most reflection events displayed in the frequency attribute are the conjugate of individual reflections originating in closely spaced reflectors with constant impedance contrasts. The reflection events

produce frequency patterns that characterize and correlate the reflectors. The frequency pattern could change as the conjugate of reflections gradually changes with thickness and lithology (Taner *et al.*, 1995). Computation of the frequency attributes may become unstable and usually noisy, with negative values exceeding the frequency range in the seismic signal (White, 1991).

The envelope amplitude attribute represents the seismic wave energy propagated through distinct geological media, where wave amplitudes increase/decrease at interfaces marking differences in acoustic impedance. Wave amplitude changes show a dependence with band width of seismic waves and the envelope amplitude attribute is quantified sample by sample along the seismic traces. The attribute varies numerically from zero to the maximum value of trace amplitude. When waves cross media from high velocity to low velocity, wave amplitude increases, and it shows as high amplitude attribute anomalies. This occurs for instance at interfaces with fluid saturation, lithological changes and distinct depositional environments with facies variation. Fractured media show as low energy zones, with bright reflectors generally absent (Taner and Sheriff, 1977).

The quality factor Q represents the ratio between wave energy over lost energy in a given oscillation cycle. It is a dimensionless factor acting as an intrinsic rock property measuring the media capacity for seismic wave energy propagation. Numerical values of Q factor depend on calculation procedure. Q factor in seismic reflection data

measures variation of the short wave length and is associated with porosity, permeability and fracturing (Taner *et al.*, 1995). Media with small Q factor values have low capacity for wave energy propagation (fractured media), whereas values close to 1 represent high capacity for wave energy propagation (Toksoz and Johnston, 1981).

RESULTS

The selected windows are located at about ~100 to 140 km (Chicx A W1) and ~30 to 70 km (Chicx A W2) in the western Chicx-A profile, and ~120 to 160 km (Chicx A1 E4) and ~40 to 75 km (Chicx A1 E3) in the eastern Chicx-A1 profile (Figure 3) with respect to the crater center. Results are summarized in Figures 5-7 for the outward and inner sections (Figure 3). The attributes correspond to (a) envelope amplitude, (b) instantaneous frequency, and (c) attenuation quality factor Q. The corresponding ranges are: 0 to 0.8 dB for envelope amplitude, 0 to 30 Hz for instantaneous frequency, and 0 to 1 for Q. Sections were selected to investigate on fracturing and deformation in the target Cretaceous rocks and major features of the crater, including the peak ring impact lithological units in the central sector, and the exterior sectors with the terrace zones (slump blocks). Depths considered down to 8 km permit to sample the Mesozoic (Cretaceous) sequences, as well as the other units in the crater area of Tertiary carbonates and

impact lithologies.

Tertiary carbonate sediments are characterized by small impedance contrasts (red colors in envelope amplitude attribute; Figure 5) and attenuation at most frequencies (red colors in instantaneous frequency attribute; Figure 6). Towards the base of the sequence and the reflectors marking the contact, impedance contrast is higher (blue colors) and instantaneous frequencies of 15 Hz or less. At around 1 km depth, instantaneous frequency anomalies show in alternating blue/yellow/red bands. Impact lithologies beneath the basin are marked by anomalies in the envelope amplitude and instantaneous frequency. The melt and basement-rich (suevite) breccias beneath the crater show higher amplitude anomalies and present greater volumes in the east than to the west. These units show frequencies less than 15 Hz (yellow and red colors). The melt and carbonate (Bunte-type) breccias do not present similar impedance contrasts; although in the flanks of the crater carbonate breccias between 200 and 900 m depths are marked by small and intermediate envelope amplitude anomalies (white color). Beneath the basin in the central part and towards the flanks, small and intermediate frequencies (between 20 and 24 Hz, green and blue colors) predominate. Higher frequencies (between 28 and 31 Hz) are associated with the carbonate breccias, particularly beneath the western peak ring. The Cretaceous carbonate sequence is characterized by small impedance contrasts. The base shows intermediate higher values (white color) marking a coherent reflector at depths of 2 to 2.5 km

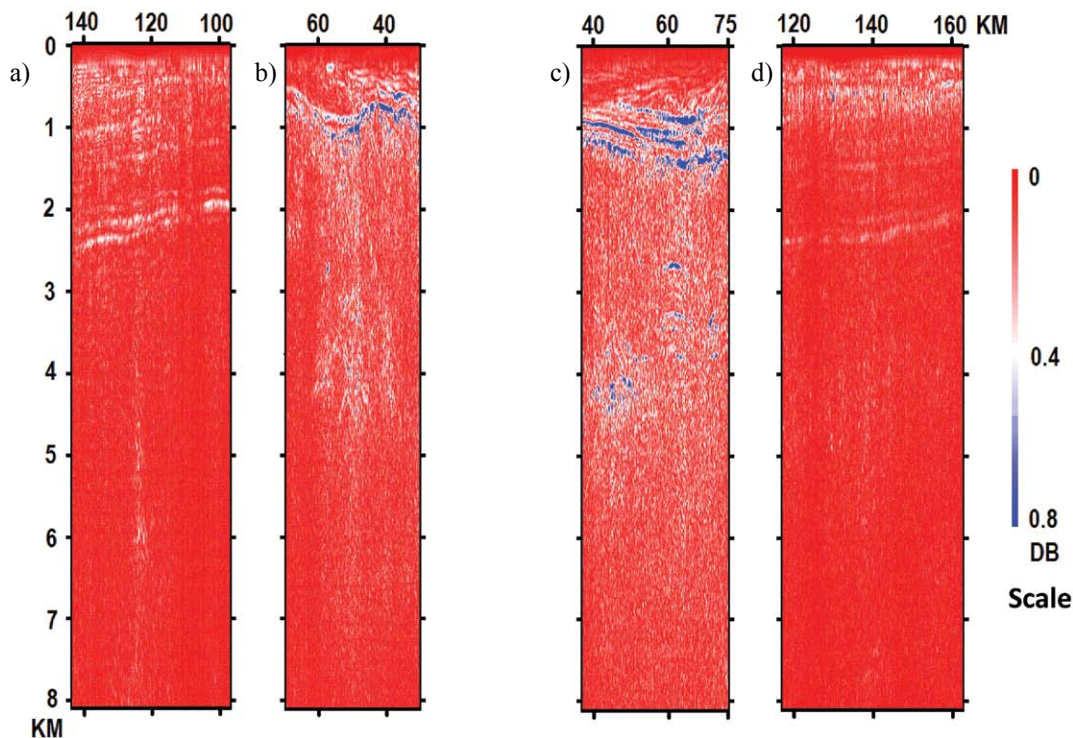


Figure 5. Envelope amplitude attribute for the seismic profile Chicx-A/A1 crossing the crater structure from west to east. Sections: a) Chicx A W1 ~100–140 km; b) Chicx A1 E4 ~120–160 km; c) Chicx A W2 ~35–65 km; and d) Chicx A1 E3 ~40–75 km. Distances with respect to crater center; see Figure 1 for location of seismic profile and Figure 3 for relative location of sections in the crater zone.

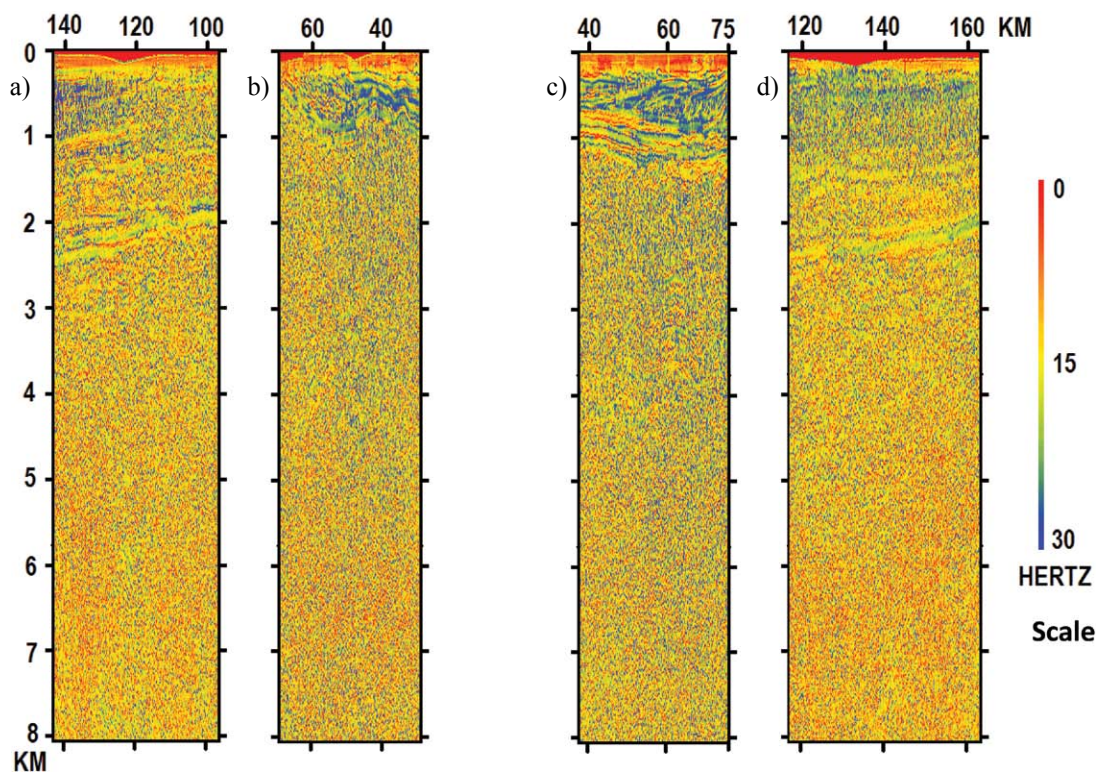


Figure 6. Frequency attribute for the seismic profile Chicx-A/A1 crossing the crater structure from west to east. Sections: a) Chicx A W1 ~100–140 km; b) Chicx A1 E4 ~120–160 km; c) Chicx A W2 ~35–65 km; and d) Chicx A1 E3 ~40–75 km. Distances with respect to crater center; see Figure 1 for location of seismic profile and Figure 3 for relative location of sections in the crater zone.

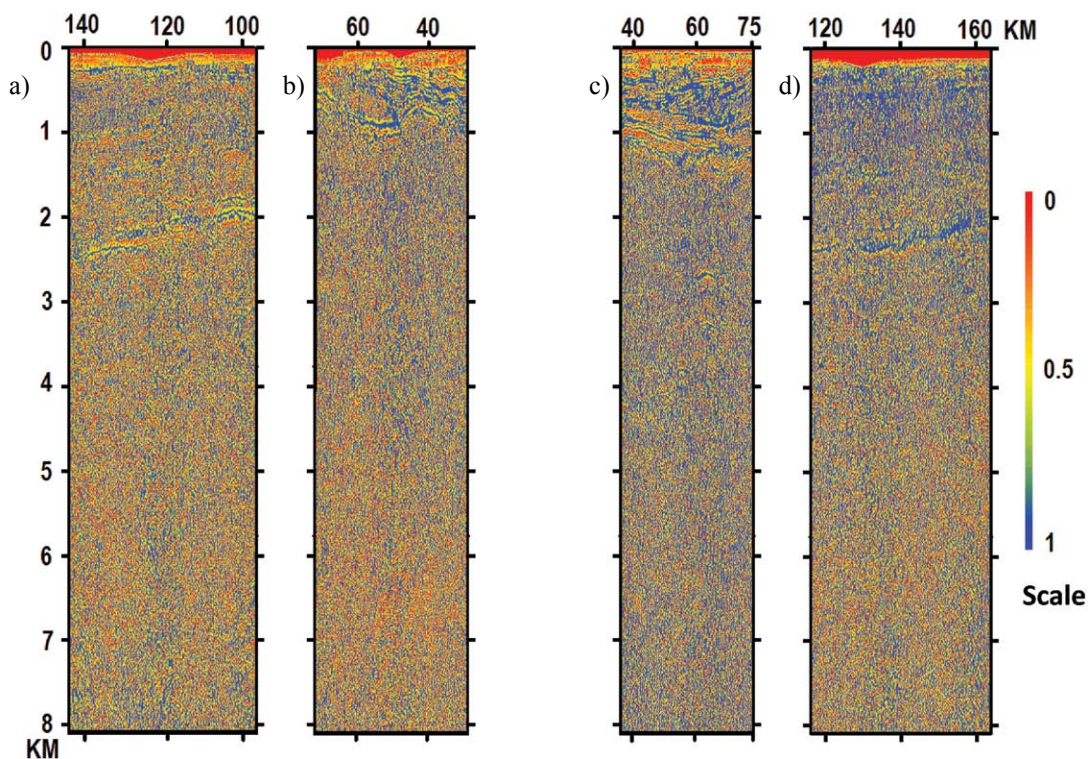


Figure 7. Attenuation quality factor attribute for the seismic profile Chicx-A/A1 crossing the crater structure from west to east. Sections: a) Chicx A W1 ~100–140 km; b) Chicx A1 E4 ~120–160 km; c) Chicx A W2 ~35–65 km; and d) Chicx A1 E3 ~40–75 km. Distances with respect to crater center; see Figure 1 for location of seismic profile and Figure 3 for relative location of sections in the crater zone.

in the exterior sectors, 100–140 km (west) and 120–160 km (east). Deeper than 2.5 km, envelope amplitude values are close to zero, showing little amplitude contrast (dominant red color).

Shock effects with shattering and fracturing of the Mesozoic target rocks decrease away from the rim zone. Besides, in the Cretaceous carbonates we observe lower attenuation inside the crater than in the exterior sectors. Results from the attenuation quality factor Q support this inference, with lower attenuation inside the crater rim than outside. Q values are small in sections outside the crater rim as compared with higher Q values inside the rim and at depth within the Cretaceous section. Sequences in the western sector (100–140 km) show larger attenuation than the eastern sector (120–160 km). Deeper units show small Q values (dominant red colors) on both exterior zones. The base of the Cretaceous sequence characterized by bright high energy reflectors show higher Q values (dominant blue colors). Direct interpretation of attenuation is however not simple. Inside the basin we have a complex arrangement of units with different lithologies, in particular impact breccias and melt, Tertiary carbonates characterized by low seismic velocities. Beneath the Tertiary basin, structural arrangement is relatively complex with units forming the peak ring, the ejecta and melt, deformation from the central uplift with fractured basement.

DISCUSSION

Modeling of complex crater morphologies with formation of central peak, peak ring and multi-ring structures has relied on hydrodynamic approaches with fluid, viscous and plastic material behavior. Fracturing and shattering of solids with finite tensile shear limits occur related to shock induced damage of target material, with fracturing and fragmentation occurring during transient cavity crater collapse processes. Studies directed to identify and characterize terrestrial impact craters show that they display distinct geophysical anomalies (Pilkington and Grieve, 1992). Geophysical studies of subsurface crater structure indicate shock-induced effects of deformation and fracturing of target rocks. Data on subsurface fracturing are limited to terrestrial craters surveyed by geophysical methods. In the 22 km diameter Ries crater, crystalline basement rocks are shattered and broken to depths of ~6 km as indicated by low densities and seismic velocities, with fractured zone beneath the crater area (Pohl *et al.*, 1977). The subsurface structure beneath the 1.2 km diameter Meteor crater displays a zone of fractured rocks extending to 1 km, which have been imaged by seismic data (Ackermann *et al.*, 1975). Shock-induced crack damage in target rocks has been studied as part of shock laboratory experiments and studies to derive models relating crater size with bolide parameters (Melosh *et al.*, 1992; Ahrens and Rubin, 1993). Experimental data indicate that damage on rock samples is restricted to impact point

zone. Xia and Ahrens (2001) report damage measured by reduction in P-wave velocity within a 15 cm-sized gabbro sample impacted with aluminum bullets at 0.8–1.2 km/s is restricted to the first 5 cm from impact point. Xia and Ahrens (2001) used depth of fractured/damage zone to derive data on cratering process and bolide parameters by using laboratory data from impacted samples and field data for the Meteor crater fractured zone.

Our analysis of shock-induced damage in the Chicxulub multi-ring crater using seismic attributes on seismic reflection profiles crossing the central part of the structure provide additional insight on the fracturing processes. Major structural features of the crater include the basin depression filled with Tertiary carbonate sediments, the peak ring, central basement uplift, the terrace zone/slump blocks and the crater, outer and exterior rings (Figure 4). The peak ring and central deformation zone beneath the Tertiary basin is related to material collapse as modeled by hydrocode simulations. Major faulting is indicated in the terrace zone, extending from beneath the peak ring to the exterior rim. Inward dipping reflectors corresponding to the crater, outer and exterior rims support fracturing and faulting during cratering. Shock effects with shattering and fracturing of the Mesozoic target rocks may decrease away from the rim zone.

Attributes provide seismic images of the major units in the crater area, permitting petrophysical characterization (differentiation) of units and unit contacts. Envelope amplitude attribute shows the Tertiary sediments with small impedance contrast (red colors), with basal sediments distinguished by higher values (blue colors) marking the base of the basin floor at 800 to 1100 m depths. High amplitude anomaly values are associated with suevitic breccias and terrace zone of slump blocks. Melt, carbonate breccias and fractured carbonates present similar values, except for carbonate breccias towards the flank of crater at some 200 to 900 m that show intermediate values (white colors). In the exterior zone, the Mesozoic carbonates show small amplitude contrasts, with major anomaly (white colors) marking the base of the Cretaceous sequence at 2 to 2.5 km depth corresponding with a bright high energy reflector package. Frequency attribute shows the Tertiary sequence with little contrasts and attenuation at most frequencies; separation into packages are marked by higher frequencies close to 30 Hz (blue colors) and towards the base sediments show frequencies less than 15 Hz. Beneath the basin, suevitic breccias are distinguished by low frequencies (less than 15 Hz, yellow and red colors). Intermediate frequencies between 20 and 24 Hz (green and blue colors) characterize the central part and around the terrace zone, probably marking the melt(?). Higher frequencies between 28 and 31 Hz correlate with the carbonate breccias in the zones beneath the western peak ring and annular central depression. Lower frequencies between 8 and 19 Hz are present in areas beneath the eastern peak ring, eastern annular depression and terrace zone. The slump blocks are distinguished by

intermediate to high frequencies (green and yellow colors). The Cretaceous sequence is characterized by intermediate to low frequencies (yellow and red colors) probably reflecting higher degrees of fracturing (see below) with the base marked by a coherent frequency anomaly with intermediate to high frequencies (yellow to green colors). Deeper units show frequencies close to zero (red colors) that characterize the deeper part of the section beneath 3 km depth.

Shock effects with shattering and fracturing of the Mesozoic target rocks decrease away from the rim zone. In the Cretaceous carbonates we observe lower attenuation inside the crater than in the exterior sectors and the crater rim is the transition zone between these two sectors. The relative attenuation quality factor Q is small in sections outside the crater rim as compared with higher Q values inside the rim, and particularly at depth within the Cretaceous section. Faulting in terrace zone is less attenuated than rim zones, possibly slump blocks are surrounded by melt and melt-rich breccias. Carbonate blocks, melt and impact breccias apparently form consolidated zones showing less attenuation as compared with other zones. Carbonate sequences in the western sector show slightly larger attenuation than in the eastern sector, suggesting radial asymmetries in fracturing/deformation within the crater. Direct interpretation is however not simple. Inside the basin, we have complex arrangements of units with different lithologies and seismic velocities, in particular the impact breccias and melt and the Tertiary carbonates characterized by low seismic velocities. Beneath the Tertiary basin, the structural arrangement is also complex with units forming the peak ring, ejecta and melt, and deformation from the central uplift and basement uplift.

ACKNOWLEDGEMENTS

Critical comments on an earlier version of the paper by two journal reviewers are gratefully acknowledged. The study forms part of the UNAM Chicxulub Research Program. Partial economic support for the study has been provided by PAPIIT grant IN-114709, CONACYT 224932, and Ixtli Digital Observatory Project.

REFERENCES

- Ackermann, H.D., Godson, R.H., Watkins, J.S., 1975, A seismic refraction technique used for subsurface investigation at Meteor crater: Arizona: *Journal of Geophysical Research*, 80, 765-775.
- Ahrens, T.J., Ruben, A.M., 1993, Impact-induced tensile failure in rock: *Journal of Geophysical Research*, 98, 1185-1203.
- Barnes, A.E., 1996, Theory of 2-D complex seismic trace analysis: *Geophysics*, 61, 264-172.
- Chopra, S., Marfurt, K.J., 2005, Seismic attributes – A historical perspective: *Geophysics*, 70, 3S0-28S0.
- Christeson, G., Nakamura, Y., Buffler, R.T., Morgan, J., Warner, M., 2001, Deep crustal structure of the Chicxulub impact crater: *Journal of Geophysical Research*, 106, 21,751-21,769.
- Collins, G.S., Morgan, J., Barton, P., Christeson, G., Gulick, S., Urrutia-Fucugauchi, J., Warner, M., Wünnemann, K., 2008, Dynamic modeling suggests terrace zone asymmetry in the Chicxulub crater is caused by target heterogeneity: *Earth and Planetary Science Letters*, 270, 221-230.
- Delgado-Rodríguez, O., Campos-Enríquez, J., Urrutia-Fucugauchi, J., Arzate, J., 2001, Occam and Bostick 1-D inversion of magnetotelluric soundings in the Chicxulub impact crater, Yucatan, Mexico: *Geofísica Internacional*, 40, 271-283.
- Del Valle-García, R., Ramírez-Cruz, L., 2002, Spectral attributes for attenuation analysis in a fractured carbonate reservoir: *The Leading Edge*, 21, 1038-1041.
- Grieve, R., Theriault, A., 2000, Vredefort, Sudbury, Chicxulub: Three of a kind?: *Annual Reviews Earth Planetary Sciences*, 28, 305-338.
- Hildebrand, A. R., Penfield, G. T., Kring, D., Pilkington, M., Camargo, A., Jacobsen, S.B., Boynton, W.V., 1991, Chicxulub Crater: A possible Cretaceous/Tertiary boundary impact crater on the Yucatan Peninsula, Mexico: *Geology*, 19, 867-871.
- Hildebrand, A.R., Pilkington, M., Ortiz-Aleman, C., Chavez, R.E., Urrutia-Fucugauchi, J., Connors, M., Graniel-Castro, E., Niehaus, D., 1998, Mapping Chicxulub crater structure with gravity and seismic reflection data, in Graddy, M.M., Hutchinson, R., McCall, G.J.H., Rotherby, D.A., (eds), *Meteorites: Flux With Time and Impact Effects: Geological Society Special Publication*, 140, 153-173.
- López-Ramos, E., 1975, Geological summary of the Yucatan peninsula, in Nairn, A.E.M., Stehli, F.G., (eds.), *The Ocean Basins and Margins*, vol. 3, *The Gulf of Mexico and the Caribbean*: New York, Plenum, 257-282.
- Melosh, H.J., 1982, A schematic model of crater modification by gravity: *Journal of Geophysical Research*, 87, 371-380.
- Melosh, H.J., 1989, *Impact Cratering: A Geologic Process*: New York, Oxford University Press, 245 pp.
- Melosh, H.J., Gaffney, E.S., 1983, Acoustic fluidization and the scale dependence of impact crater morphology: *Journal of Geophysical Research*, 88, Supplement, A830-A834.
- Melosh, H.J., Ivanov, B.A., 1999, Impact crater collapse: *Annual Reviews Earth Planetary Sciences*, 385-415.
- Melosh, H.J., Ryan, E.V., Aspaug, E., 1992, Dynamic fragmentation in impacts: Hydrocode simulation of laboratory impacts: *Journal of Geophysical Research*, 97, 14,735-14,759.
- Morgan, J., Warner, M., 1999, Chicxulub: The third dimension of a multi-ring basin: *Geology*, 27, 407-410.
- Morgan, J., Warner, M., Chicxulub Working Group, 1997, Size and morphology of the Chicxulub impact crater: *Nature*, 390, 472-476.
- Morgan, J., Christeson, G., Zelt, C., 2002, Testing the resolution of a 3D velocity tomogram across the Chicxulub crater: *Tectonophysics*, 355, 215-226.
- O'Keefe, J.D., T.J. Ahrens, 1999, Complex craters: Relationship of stratigraphy and rings to impact conditions: *Journal of Geophysical Research*, 104, 27,091-27,104.
- Ortiz-Alemán, C., Urrutia-Fucugauchi, J., 2010, Aeromagnetic anomaly modeling of central zone structure and magnetic sources in the Chicxulub crater: *Physics of the Earth and Planetary Interiors*, doi:10.1016/j.pepi.2010.01.007.
- Pilkington, M., Grieve, R.A.F., 1992, The geophysical signature of terrestrial impact craters: *Reviews of Geophysics*, 30, 161-181.
- Pohl, J., Stoffler, D., Gall, H., Ernstson, K., 1977, The Ries crater, in Roddy D.J., Pepin, R.O., Merrill, R.B. (eds.), *Impacts and Explosion Cratering*: New York, Pergamon Press, 343-404.
- Ramírez-Cruz, L., del Valle-García, R., Urrutia-Fucugauchi, J., 2005, Enhanced oil production in a mature field assisted by spectral attenuation analysis: *Journal of Geophysics and Engineering*, 2, 48-53.
- Rebolledo-Vieyra, M., Urrutia-Fucugauchi, J., 2006, Magnetostratigraphy of the Cretaceous/Tertiary boundary and early Paleocene sedimentary sequence from the Chicxulub impact crater: *Earth Planets Space*, 58, 1309-1314.
- Rebolledo-Vieyra, M., Urrutia-Fucugauchi, J., Marin, L., Trejo, A., Sharpton, V., Soler, A.M., 2000, UNAM scientific shallow-drilling program of the Chicxulub impact crater: *International Geology*

- Review, 42, 928-940.
- Sharpton, V.L., Dalrymple, G., Marin, L., Ryder, G., Schuraytz, B., Urrutia-Fucugauchi, J., 1992, New links between the Chicxulub impact structure and the Cretaceous/Tertiary boundary: *Nature*, 359, 819-821.
- Sharpton, V.L., Burke, K., Camargo, A., Hall, S.A., Lee, S., Marin, L., Suarez, G., Quezada, J.M., Spudis, P.D., Urrutia-Fucugauchi, 1993, Chicxulub multiring impact basin: Size and other characteristics derived from gravity analysis: *Science*, 261, 1564-1567.
- Sheriff, R.E., 1991, *Encyclopedic Dictionary of Exploration Geophysics*, SEG, Tulsa, USA.
- Taner, M.T., Sheriff, R.E., 1977, Application of amplitude, frequency and other attributes to stratigraphic and hydrocarbon determination, in Payton C.E. (ed), *Applications to Hydrocarbon Exploration*, AAPG Memoir 26: Tulsa, American Association of Petroleum Geologists, 301-327.
- Taner, M.T., Koehler, F., Sheriff, R.E., 1979, Complex seismic trace analysis: *Geophysics*, 44, 6, 1041-1063.
- Taner, M., Schuelke, J. S., O'Doherty, R., Baysal, E., 1995, Seismic attributes revisited, in 64th Annual International Meeting of the Society of Exploration Geophysicists, Expanded Abstracts, 1104-1106.
- Toksoz, N., Johnston, D., 1981, *Seismic Wave Attenuation*: Tulsa Oklahoma, USA, Society of Exploration Geophysicists, 459 pp.
- Urrutia-Fucugauchi, J., Pérez-Cruz, L., 2008, Post-impact carbonate deposition in the Chicxulub impact crater region, Yucatan platform, Mexico: *Current Science*, 95, 241-252.
- Urrutia-Fucugauchi, J., Perez-Cruz, L., 2009, Multiring-forming large bolide impacts and evolution of planetary surfaces: *International Geology Review*, 51, 1079-1102. doi: 10.1080/002068 10902867 161.
- Urrutia-Fucugauchi, J., Marin, L., Sharpton, V.L., 1994, Reverse polarity magnetized melt rocks from the Cretaceous/Tertiary Chicxulub structure, Yucatan peninsula, Mexico: *Tectonophysics*, 237, 105-112.
- Urrutia-Fucugauchi, J., Marin, L., Trejo-Garcia, A., 1996, UNAM scientific drilling program of Chicxulub impact structure: Evidence of a 300-km crater diameter: *Geophysical Research Letters*, 23, 1565-1568.
- Urrutia-Fucugauchi, J., Morgan, J., Stoeffler, D., Claeys, P., 2004, The Chicxulub Scientific Drilling Project: *Meteoritics and Planetary Science*, 39, 787-790.
- Urrutia-Fucugauchi, J., Chavez-Aguirre, J.M., Pérez-Cruz, L., de la Rosa, J.L., 2008, Impact ejecta and carbonate sequence in the eastern sector of Chicxulub crater: *Comptes Rendus Geosciences*, 341, 801-810.
- White, R.E., 1991, Properties of instantaneous seismic attributes: *The Leading Edge*, 7, 26-32.
- Xia, K., Ahrens, T.J., 2001, Impact induced damage beneath craters: *Geophysical Research Letters*, 28, 3525-3527.

Manuscript received: July 20, 2008

Corrected manuscript received: August 12, 2009

Manuscript accepted: November 23, 2009